Integrating Static and Dynamic Load Analysis for Optimized Bottom Frame Design in Industrial Machine Applications

Bondan Wiratmoko Budi Santoso [1*], Nayo Kenny Giovanni [2], Daniel Gilang Nuzullian [3], Andreas Sugijopranoto [4], Yotam Stefanditya [5], Paulinus Cherlyndo Paterias [6], Winastwan Sista Hayu [7], Abram Pangeling [8], Deslana Avinda Krisna Putra [9] Bayu Prabandono [10]

[1, 2, 3, 4,5] Perancangan Manufaktur, Politeknik ATMI Surakarta, Surakarta, Indonesia

Email: [1*] bondanwiratmoko69@gmail.com, [2] nkgiovanni02@gmail.com, [3] danielgilangnuzullian@gmail.com, [4] andre@atmi.ac.id, [5] yotam.stefanditya@atmi.ac.id, [6] cherlyndo.paterias@atmi.ac.id, [7] sista.hayu@atmi.ac.id, [8] abram.pangeling@atmi.ac.id, [9] deslana.putra@atmi.ac.id, [10] bayu.prabandono@atmi.ac.id

*Corresponding Author

Abstract— **The objective of this study was to comparatively analyze the strength and stress distribution of three bottom frame design variations of the Bandrole machine. This analysis was conducted using both static and dynamic load analyses, which were based on Computer-Aided Engineering (CAE). The three variations included the original manufacturer's bottom frame (Design 1), a modified frame with an additional footplate (Design 2), and a modified frame with reinforced side walls (Design 3). The dynamic simulation results demonstrated that Design 2 yielded the maximum force of 6321.06 N, accompanied by a 16.146% increase in load. Concurrently, the static analysis revealed that Design 2 manifested the lowest Von Mises stress (13.76 MPa) and minimal deformation (0.0154 mm), thereby confirming its status as the optimal design. Furthermore, testing under different rotational speeds (400–600 rpm) confirmed the stability of Design 2, with only minor changes in stress and deformation observed. The findings of this study yielded recommendations for enhancing the reliability of machine design, which could serve as a benchmark for the future development of analogous machine structures.**

Keywords— CAE; Static analysis; Dynamic analysis; Frame design; Stress distribution; Machine reliability

I. INTRODUCTION

The rapid advancements in modern manufacturing technology have led to increasing demands for enhanced efficiency and structural reliability in industrial machinery components, particularly in the load-bearing frameworks that support dynamic operations. In machines utilized for high-speed production, such as the cigarette banding machines, the structural integrity and rigidity of the bottom frame are foundational elements in ensuring operational accuracy, vibration resistance, and overall service life [1], [2], [3], [4]. As asserted by Beer and Johnston [5], inadequate frame design frequently gave rise to localized stress concentrations, which in turn resulted in excessive deformation and performance degradation. The aforementioned phenomena occurred as a consequence of the combined effects of both static and dynamic loads during the operational cycle [6], [7], [8].

Recent developments in Computer-Aided Engineering (CAE) have enabled engineers to virtually evaluate and optimize the structural behavior of machine components prior to manufacturing [9], [10], [11], [12], [13]. CAE-based simulations facilitate detailed analyses of stress distribution, deformation patterns, and the overall response of mechanical structures under varying load and rotational conditions [6], [11], [14], [15]. Within the packaging industry, where bandrole machines operate under continuous, high-speed, and repetitive cycles, CAE has become a crucial tool to ensure long-term stability and prevent structural fatigue or failure [16], [17].

Previous research has extensively utilized finite element methods (FEM) to study the structural integrity of industrial machinery frames. However, most investigations have focused on macro-structural elements such as the main frame or housing rather than the bottom frame, which directly absorbs vibrations and mechanical forces generated by the machine’s operating mechanism [18], [19], [20]. Moreover, limited comparative analyses exist that evaluate the effects of different bottom frame design variations under both static and dynamic loading [21], [22], [23], [24], [25], particularly for the cigarette banding machines, which operates at relatively high rotational speeds ranging from 400 to 600 rpm.

The structural limitations exhibited by the bottom frame of the cigarette banding machine were attributable to inadequate stiffness, uneven stress distribution, and excessive deformation under combined static and dynamic loading conditions. These deficiencies had the potential to reduce operational stability, accelerate fatigue, and compromise the machine's long-term performance [26], particularly at higher rotational speeds commonly required in industrial applications. However, previous studies had rarely focused on the comparative evaluation of bottom-

Received: 21-10-2025
Revised: 20-11-2025
Published: 31-12-2025

frame design variations, leaving uncertainty regarding which geometric configuration could deliver optimal mechanical strength and dynamic reliability. Consequently, a systematic investigation was necessary to assess how different bottom-frame designs responded to operational forces and to identify a configuration capable of improving structural integrity and machine durability [27], [28].

In response to these research gaps, the present study aims to perform a comparative analysis of the strength and stress distribution in three design variations of the Bandrole machine's bottom frame using static and dynamic load simulations within a CAE environment. The evaluated configurations include: (1) the original manufacturer's bottom frame, (2) a modified frame with an additional footplate, and (3) a reinforced frame with strengthened side walls. Through numerical simulations, this study seeks to identify the most optimal configuration that provides superior rigidity, minimal deformation, and uniform stress distribution under varying operational conditions [29], [30]. The findings are expected to contribute valuable insights for enhancing the design reliability and mechanical performance of similar industrial machine structures in future applications [31], [32], [33].

II. METHOD

The focal point of this research was the cigarette banding machines, which served as the foundation for the comparative structural analysis conducted in this study. The machine was selected due to its critical role in the packaging process and the frequent occurrence of frame-related structural issues that affect its operational stability and reliability. The investigation was undertaken to ascertain the impact of design modifications on mechanical performance. To this end, three distinct bottom-frame design variants were developed and analyzed.

The initial variant, designated as Design 1, represented the original frame configuration produced by the manufacturer and served as the baseline reference model. The second variant, designated Design 2, incorporated a modified frame equipped with an additional footplate. This modification was designed to enhance load distribution and reduce stress concentration at the base junctions. The third variant, designated Design 3, featured reinforced side walls with the objective of enhancing lateral stiffness and minimizing deformation under operational loading conditions. The three design variations were shown in Fig. 1.

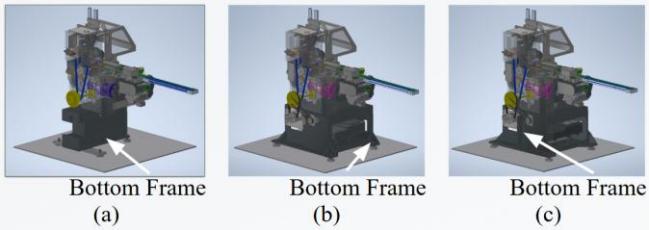

Fig. 1. (a) Design 1: Factory-built frame; (b) Design 2: Modified footplate; (c) Design 3: Modified frame wall.

The three frame designs were modeled using Computer-Aided Design (CAD) software (Autodesk Inventor), ensuring dimensional consistency and accurate geometric representation. Subsequently, the models were exported to Computer-Aided Engineering (CAE) software for conducting both static and dynamic load analyses. This process enabled the assessment of stress distribution, deformation characteristics, and overall structural integrity under simulated operating conditions that represented real machine dynamics.

The following flowchart (Fig.2), illustrated the sequence of the research that was conducted.

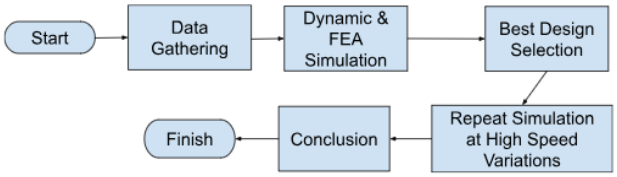

Fig. 2. flowchart.

A. *Dynamic Simulation*

To validate the analysis, each model was subjected to identical boundaries conditions, material properties, and load magnitudes. The material used in this study was Carbon Steel. The steel was characterized by a Young's modulus of 200 GPa and a Poisson's ratio of 0.29. The material also exhibited a typical yield strength in the range of 350 MPa and an ultimate tensile strength of 420 Mpa, depending on the grade referenced within the software library. These standardized values were implemented to ensure consistency in the numerical simulation and to reflect the default isotropic mechanical behavior defined in Autodesk Inventor. Moreover, the simulation parameters—including mesh density, element type, and constraint configuration—were standardized across all models to ensure the comparability of results. These analyses yielded quantitative insights into the mechanical performance and stability of each design variation, providing a foundation for determining the optimal configuration of the cigarette banding machines bottom frame.

Simulation procedure:

1. Determination of kinematic joints on moving components.
2. Assignment of parameters: gravity and angular velocity of 36.65 rad/s (equivalent to 350 RPM).
3. Tracking of component motion using the trace feature (Fig. 3 and 4).
4. Extraction of reaction force data for FEA analysis.

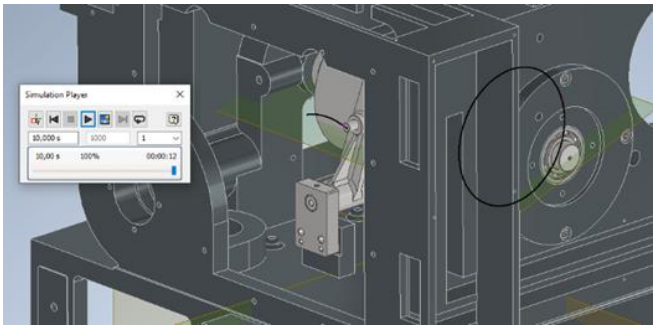

Fig. 3. Simulation cycle parameters.

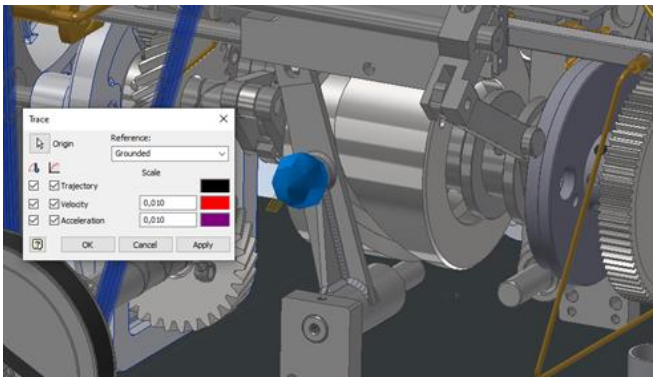

Fig. 4. Trace application.

The dynamic analysis conducted in this study was classified as a transient dynamic analysis because the simulation evaluated the time-dependent response of the structure under rotational excitation rather than determining its natural frequencies. The model was subjected to prescribed angular velocities, and the resulting reaction forces were extracted as functions of time. This approach is consistent with conventional transient analysis, which assesses structural behavior under non-steady, time-varying loads. This study did not perform eigenvalue extraction or mode-shape identification, which are characteristic of modal analysis. Consequently, the dynamic assessment relied on transient response data to generate the input loads for subsequent finite element evaluation, providing a realistic representation of operational machine dynamics.

B. Finite Element Analysis (FEA)

The material used in this study was cast iron. It was characterized by a Young's modulus of 120.5 GPa and a Poisson's ratio of 0.30. It also exhibited typical yield and ultimate tensile strengths of 758 and 884 MPa, respectively.

Simulation procedure:

1. The mesh model was created using pyramid (tetrahedral) elements with densification in areas that experienced high concentration.
2. The load input was obtained from the results of the dynamic simulation.

C. Analysis Parameters

1. Stage 1 : Test three designs at a constant speed

TABLE I. STAGE 1 TABLE TEMPLATE

No	Description	Analysis Results Design 1	Analysis Results Design 2	Analysis Results Design 3
1	*Max Force* (N)			
2	*Von Mises Stress* (MPa)			
3	*Displacement* (mm)			

2. Stage 2: Test the selected (best) design with speed variations of 400, 450, 500, 550, and 600 RPM. Record the results in a table template as shown in Table 2

TABLE II. STAGE 2 TABLE TEMPLATE

No	Analysis Results	400 RPM	450 RPM	500 RPM	550 RPM	600 RPM
1	Max Force (N)					
2	Von Mises Stress (MPa)					
3	Displacement (mm)					

D. Expected Results

Recommendations for underframe design with :

1. Minimum Von Mises stress
2. Lowest displacement
3. Stable speed variation

III. RESULTS AND DISCUSSION

A. Results of Stage 1 Analysis

Dynamic simulation at 350 RPM (36.65 rad/s) shows:

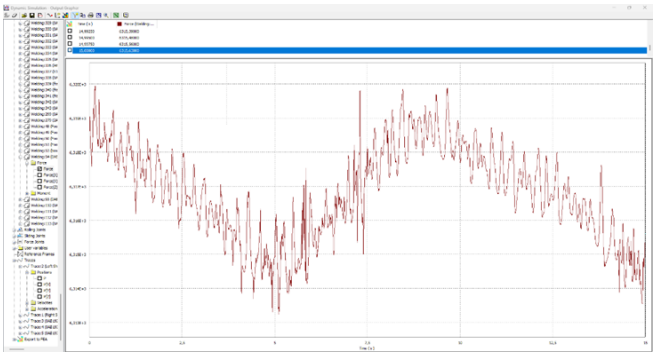

Fig. 5. Results of stage 1 Dynamic Simulation Design 1.

Fig. 5 Shows the dynamic simulation results in Stage 1 of Design 1. Based on the simulation results graph for design 1, a maximum force of 6319.95 N was obtained at 0.155 seconds.

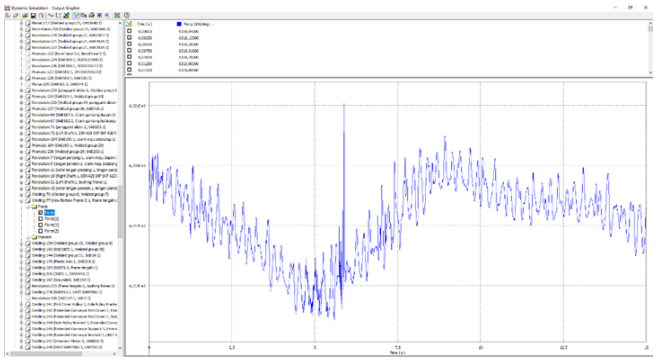

Fig. 6. Results of stage 1 Dynamic Simulation Design 2.

Fig. 6 Shows the dynamic simulation results in Stage 1 of Design 2. Based on the simulation results graph for design 2, a maximum force of 6321.06 N was obtained at 5.885 seconds.

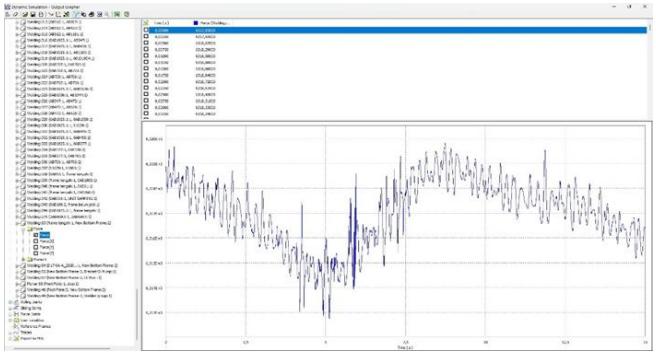

Fig. 7. Results of stage 1 Dynamic Simulation Design 3.

Fig. 7 Shows the dynamic simulation results in Stage 1 of Design 3. Based on the simulation results graph for design 3, a maximum force of 6319.82 N was obtained at 8.7425 seconds.

Key findings:

1. Stress concentration:
   - Design 1: Concentrated at the steel plate joint (Fig. 5).

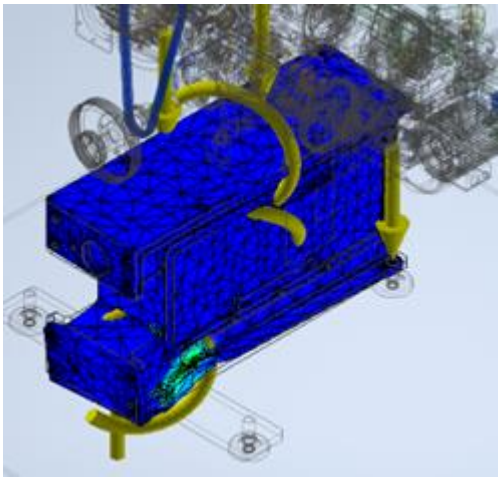

Fig. 8. Results of stage 1 Static Simulation Design 1.

   - Design 2: Spread across the oil pan area (Fig. 6).

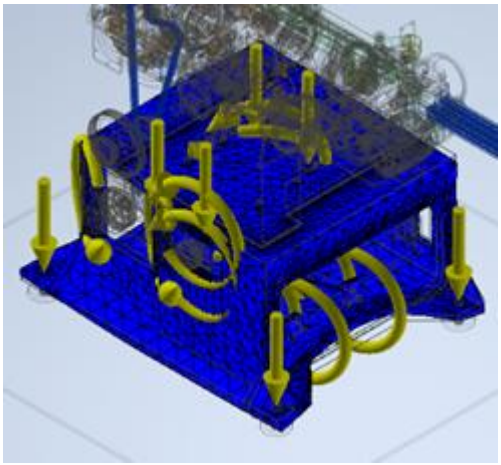

Fig. 9. Results of stage 1 Static Simulation Design 2.

   - Design 3: Concentrated at the leg joints (Fig. 7).

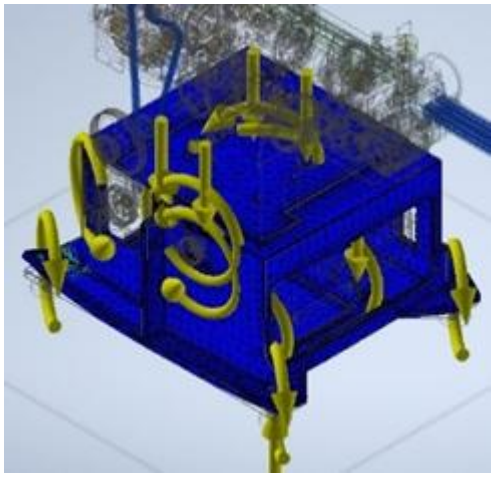

Fig. 10. Results of stage 1 Static Simulation Design 3.

The results of the dynamic simulation followed by the static simulation are summarized in Table III.

TABLE III. STAGE 1 SIMULATION RESULTS

No	Description	Analysis Results Design 1	Analysis Results Design 2	Analysis Results Design 3
1	*Max Force* (N)	6319.95	6321.06	6319.82
2	*Von Mises Stress* (MPa)	17.91	13.76	29.76
3	*Displacement* (mm)	0.0258	0.0154	0.124

2. Design 2 shows the best performance with:
   - Stress 23% lower than Design 1.
   - Displacement 40% smaller than Design 1.

B. Results of Stage 2 Analysis

Design 2 was subjected to testing at elevated rotational speeds, surpassing 350 RPM, to assess the structural integrity of the machine's bottom frame. This evaluation was conducted to anticipate future developments aimed at enhancing production capacity, which would, in turn, elevate the machine's operating RPM. In this experiment, rotational speeds were set between 400 and 600 RPM, with 50 RPM intervals, as planned in Table 2.

TABLE IV. STAGE 2 SIMULATION RESULTS

No	Analysis Results	400 RPM	450 RPM	500 RPM	550 RPM	600 RPM
1	Max Force (N)	6320.71	6321.51	6320.56	6321.25	6321.41
2	Von Mises Stress (MPa)	13.76	13.76	13.76	13.76	13.78
3	Displacement (mm)	0.01540	0.01540	0.01540	0.01540	0.01547

Advantages of "Design 2":

- More even stress distribution.
- The addition of motor mounts and oil pans improves structural strength.
- Consistent performance across speed variations.

Limitations (notes taken during the simulation computation process): The model was simplified by removing chamfers and combining standard components.

Design 2 is recommended for implementation because:

- It meets the safety factors for cast iron (stress <150 Mpa).
- It maintains stability under extreme operating conditions (+71% normal Rpm).

The comprehensive static and dynamic analyses carried out in this study provided several convergent lines of evidence that supported the superiority of Design 2 for the Bandrole machine bottom frame. The findings indicated that Design 2 demonstrated the lowest Von Mises stress (13.76 MPa) and the smallest displacement (0.0154 mm) among the three alternatives, suggesting enhanced global stiffness and more advantageous load-path distribution. This behavior was consistent with the principles of topology and geometry-based optimization, where the addition of small but targeted geometry elements—such as the additional footplate—significantly altered the flow of reaction forces through the structure and consequently reduced peak stress concentrations. According to the findings of previous studies that combined geometry refinement and topology-aware design, there was a notable decrease in localized stress and an enhancement in stiffness-to-mass performance. These design modifications were particularly effective when applied along principal load paths as opposed to when employed as isolated stiffening elements [12], [13], [29], [34].

Another salient observation was the dynamic robustness of Design 2 across the tested rotational spectrum (400–600 RPM). The nearly constant values of Von Mises stress and displacement with speed variation suggested that the structure's modal characteristics did not approach resonance with the excitation harmonics produced under simulated operating conditions. In machine-frame design, the avoidance of resonance was imperative, as a natural frequency that approximated the excitation frequency could substantially amplify the dynamic response and expedite fatigue damage [6], [7], [34], [33]. The observed stability in the CAE results thus indicated that the fundamental flexural and torsional modes of the redesigned underframe remained well separated from the machine's operating frequencies—a finding consistent with prior experimental modal analyses and dynamic simulations of machine tools and rotating machinery [7], [11].

A thorough examination of the stress maps revealed that Design 1 exhibited stress concentration at the plate joints, while Design 3 demonstrated stress concentration at the leg joints, thereby unveiling disparate failure-prone mechanisms. The stress concentration observed at the plate joint of Design 1 is likely attributable to sudden fluctuations in cross-sectional stiffness, which functioned as local stress amplifiers. Concurrently, the augmented sidewalls of Design 3 engendered stiffness discrepancies, thereby redistributing stress to the leg-root regions. This phenomenon resulted in augmented displacement and diminished global stiffness. This outcome aligns with the observations reported by Zhao et al. [21] and Krtinić et al. [18], who demonstrated that improper alignment or over-stiffening of reinforcements can lead to the formation of secondary load paths and stress risers. Conversely, Design 2 exhibited superior outcomes, suggesting that optimizing the base reinforcement, as opposed to merely thickening the side walls, constitutes a more efficacious and direct approach to augmenting frame stability and rigidity [20], [22].

From the perspective of fatigue and life-prediction analysis, the stress distribution exhibited by Design 2 was found to be advantageous due to its uniformity. The phenomenon of fatigue crack nucleation was predominantly observed in regions exhibiting elevated levels of cyclic stress and pronounced stress concentration factors. Despite the fact that the overall stress levels remained well below the static yield strength of structural steel, cyclic loading under repetitive operation had the potential to initiate microcracks even at low stresses, provided that the concentration factor was high. Recent hybrid approaches combining finite element analysis and data-driven fatigue modeling have confirmed that uniform stress distribution and reduced stress peaks are the most effective methods to extend component life [3], [36], [37]. Consequently, the enhancements accomplished by Design 2 were anticipated to generate quantifiable enhancements in the long-term reliability and service life of the machine's structural components.

The trade-off between model fidelity and computational practicality also emerged as an important issue. The study implemented geometric simplifications, including the omission of chamfers, the combination of standard parts, and the idealization of welds and bolts. These simplifications were necessitated by hardware constraints but may have influenced local stress predictions. Conventional wisdom among researchers in this field posits that the accurate modeling of joints, fasteners, and weld toes has a substantial impact on the stress distribution outcomes in finite element simulations [18], [37], [36]. Consequently, while the comparative ranking of the three designs was deemed reliable, the prediction of exact fatigue life and localized failure risks would necessitate more detailed submodeling of joint regions in subsequent research.

From an engineering and manufacturing perspective, the design modification introduced in Design 2 represented a cost-effective improvement. The incorporation of an additional footplate and the optimization of the motor mount resulted in structural benefits that could be achieved with minimal alterations to the prevailing fabrication processes. In comparison with extensive wall reinforcements, this modest yet deliberate modification has been shown to reduce stress and deformation while maintaining ease of manufacture and assembly. This design approach was aligned with the principles of "small-geometry, high-impact" optimization, which offered significant mechanical improvements without increasing production complexity or costs [30], [31]. This approach has also been observed in industrial retrofitting practices, where targeted modifications are preferred over complete structural redesigns to improve performance while minimizing downtime and expenses [32], [33].

Another critical dimension involved the integration of digital verification tools beyond static and dynamic simulations. Contemporary CAE methodologies have seen an increased incorporation of model-updating techniques that are informed by experimental data. This development serves to bridge the gap between numerical predictions and the actual machine behavior [6], [30], [29]. Researchers such as Lin et al. [39] demonstrated that finite element models corrected by measured dynamic responses produced much higher accuracy in predicting machine behavior under variable loading. The implementation of a feedback-based model correction technique on the bottom frame of the Bandrole machine would have further enhanced the predictive accuracy and facilitated the identification of potential resonant conditions under future operational configurations.

Furthermore, the potential for additional optimization exists through the integration of topology optimization with additive manufacturing processes. Machine - learning - assisted topology optimization and heterogeneous lattice structure design techniques have been demonstrated to enhance stiffness while reducing overall weight [28], [33], [32]. Although the present frame was conventionally fabricated from steel plates, integrating these methods in future prototypes could enable lightweight yet rigid structures capable of improved damping. The efficacy of these techniques has been demonstrated in the domains of press machine frames and composite manufacturing systems, thereby substantiating their adaptability to diverse mechanical structures [12], [18].

The implementation of advanced sensing technologies has also facilitated avenues for continuous performance verification. The integration of accelerometers or optical sensors for vibration monitoring could facilitate real-time validation of CAE predictions and early detection of dynamic deviations [1], [39], [38]. In particular, vision-based vibrometry has been demonstrated to be an effective method for non-contact assessment of vibration modes in machine tools [41] [39]. The incorporation of these sensors within the Bandrole apparatus could potentially enable the implementation of predictive maintenance methodologies. This would be achieved by identifying shifts in modal frequency or unexpected vibration amplitudes, which are often indicative of developing structural issues.

Finally, when the findings of this study were considered within the broader context of industrial design optimization, the research demonstrated a structured pathway from simulation-based insight to manufacturable improvement. The integration of static and dynamic simulations, supplemented by CAE verification, signified an inaugural stride toward digital twin frame [42], [43], [44], which have the potential to facilitate condition-based maintenance and lifecycle management of production equipment[31], [32], [33]. The proposed sequence for subsequent implementation included the adoption of Design 2 as the new baseline, the conducting of operational modal tests on pilot machines, the application of model-updating procedures using collected field data, and the integration of fatigue submodels for joint regions. Such a sequence was expected to transform the CAE-driven analysis into a validated, data-supported improvement cycle, bridging simulation and real-world operation in line with current Industry 4.0 design methodologies [39] [37].

IV. CONCLUSION

The integration of dynamic and static simulations yielded a comprehensive understanding of the structural performance of the cigarette banderole machine's bottom frame, thereby enabling effective problem-solving and design optimization. Among the three configurations, "Design 2" demonstrated the optimal performance, exhibiting the highest load capacity (6321.06 N) with uniform stress distribution and minimal deformation (0.0154 mm). It maintained stability up to 600 RPM, exhibiting negligible stress and deformation increases. The combined simulation approach was advantageous in exploring a wider range of design alternatives by manipulating multiple variables, thus enhancing the robustness of the design evaluation process. However, the analysis was constrained by hardware limitations, as high computational capacity was essential to accommodate the required accuracy and detail. A comprehensive evaluation of the configurations revealed that Design 2 was identified as the most feasible and optimal configuration for operational implementation. The

study recommended the initiation of future studies to focus on performance enhancement at higher rotational speeds and the advancement of computational resources to support more complex simulations.

ACKNOWLEDGMENT

The authors conveyed their profound gratitude to Politeknik ATMI Surakarta for its provision of the research facilities, technical support, and computational resources indispensable for the successful execution of this study. Additionally, appreciation was expressed to the Manufacturing Design Department and the CAE Laboratory team for their invaluable assistance in conducting simulations and data analysis. The authors acknowledged the constructive feedback and academic guidance provided by advisors and colleagues. This feedback contributed substantially to the enhancement of this research.

REFERENCE

[1] R. G. Budynas, J. K. Nisbett, and J. E. Shigley, Shigley's mechanical engineering design, Eleventh edition in SI units. New York, NY: McGraw-Hill, 2021.

[2] K. Charoensuk and T. Sethaput, "The Vibration Analysis Based on Experimental and Finite Element Modeling for Investigating the Effect of a Multi-Notch Location of a Steel Plate," Applied Sciences, vol. 13, no. 21, p. 12073, Nov. 2023, doi: 10.3390/app132112073.

[3] Y. Wang, Y. Ma, and J. Hong, "Study on dynamic stiffness of supporting structure and its influence on vibration of rotors," Chinese Journal of Aeronautics, vol. 35, no. 11, pp. 252–263, Nov. 2022, doi: 10.1016/j.cja.2022.01.017.

[4] A. Sharma, S. Thapa, B. Goel, R. Kumar, and T. Singh, "Structural analysis and optimization of machine structure for the measurement of cutting force for wood," Alexandria Engineering Journal, vol. 64, pp. 833–846, Feb. 2023, doi: 10.1016/j.aej.2022.09.030.

[5] F. P. Beer, E. R. Johnston, J. T. DeWolf, and D. F. Mazurek, Eds., Mechanics of materials, 7. ed. New York, NY: McGraw-Hill Education, 2015.

[6] J. Berthold, M. Kolouch, J. Regel, and M. Dix, "Identification of natural frequencies of machine tools during milling: comparison of the experimental modal analysis and the operational modal analysis," Prod. Eng. Res. Devel., Apr. 2024, doi: 10.1007/s11740-024-01270-6.

[7] M. Law, P. Gupta, and S. Mukhopadhyay, "Modal analysis of machine tools using visual vibrometry and output-only methods," CIRP Annals, vol. 69, no. 1, pp. 357–360, 2020, doi: 10.1016/j.cirp.2020.04.043.

[8] Z.-W. Zhuang, J.-C. Lu, and D.-S. Liu, "A novel identification technique of machine tool support stiffness under the variance of structural weight," Int J Adv Manuf Technol, vol. 119, no. 1–2, pp. 247–259, Mar. 2022, doi: 10.1007/s00170-021-08257-y.

[9] T. R. Chandrupatla, A. D. Belegundu, and T. Ramesh, Introduction to finite elements in engineering, 4. ed., International ed. in Always learning. Upper Saddle River, NJ: Pearson, 2012.

[10] A. Cornaggia, D. Mrówczyński, T. Gajewski, A. Knitter-Piątkowska, and T. Garbowski, "Advanced Numerical Analysis of Transport Packaging," Applied Sciences, vol. 14, no. 24, p. 11932, Dec. 2024, doi: 10.3390/app142411932.

[11] Y. Zhang et al., "Accurate Finite Element Simulations of Dynamic Behaviour: Constitutive Models and Analysis with Deep Learning," Materials, vol. 17, no. 3, p. 643, Jan. 2024, doi: 10.3390/ma17030643.

[12] Z. Tong, C. Shen, J. Fang, M. Ding, and H. Tao, "Research on the Application of Structural Topology Optimisation in the High-Precision Design of a Press Machine Frame," Processes, vol. 12, no. 1, p. 226, Jan. 2024, doi: 10.3390/pr12010226.

[13] D. Zhao and H. Wang, "Topology Optimization of Compliant Mechanisms Considering Manufacturing Uncertainty, Fatigue, and Static Failure Constraints," Processes, vol. 11, no. 10, p. 2914, Oct. 2023, doi: 10.3390/pr11102914.

[14] C. Zhang, G. Jin, Z. Wang, and Y. Sun, "Dynamic stiffness formulation and vibration analysis of coupled conical-ribbed cylindrical-conical shell structure with general boundary condition," Ocean Engineering, vol. 234, p. 109294, Aug. 2021, doi: 10.1016/j.oceaneng.2021.109294.

[15] A. Max, M. Hynek, and L. Řehounek, "DYNAMIC ANALYSIS OF CNC MILLING MACHINE FRAME".

[16] J. McLeish and N. Blattau, "CAE apps for Physics of Failure reliability & durability simulations," in 2014 Reliability and Maintainability Symposium, Colorado Springs, CO, USA: IEEE, Jan. 2014, pp. 1–6. doi: 10.1109/RAMS.2014.6798444.

[17] "Fatigue Life Prediction of a Bus Body Structure Using CAE Tools".

[18] N. Krtinić, M. Marinković, and M. Gams, "Finite Element Method Analysis of Seismic Response of Confined Masonry Walls with Openings Built Using Polyurethane Glue," Buildings, vol. 15, no. 3, p. 424, Jan. 2025, doi: 10.3390/buildings15030424.

[19] M. Song, Z. Wang, X. Chen, B. Liu, S. Huang, and J. He, "Numerical Investigation of Progressive Collapse Resistance in Fully Bonded Prestressed Precast Concrete Spatial Frame Systems with and Without Precast Slabs," Buildings, vol. 15, no. 15, p. 2743, Aug. 2025, doi: 10.3390/buildings15152743.

[20] M. Krawczuk and M. Palacz, Eds., Applications of Finite Element Modeling for Mechanical and Mechatronic Systems. Basel, Switzerland: MDPI - Multidisciplinary Digital Publishing Institute, 2021.

[21] M. Zhao, G. Wu, and K. Wang, "Comparative Analysis of Dynamic Response of Damaged Wharf Frame Structure under the Combined Action of Ship Collision Load and Other Static Loads," Buildings, vol. 12, no. 8, p. 1131, July 2022, doi: 10.3390/buildings12081131.

[22] V. C. S. Cuajao, "COMPARISON OF STATIC AND DYNAMIC LOAD TESTING: A REVIEW," GEOMATE, vol. 27, no. 121, Sept. 2024, doi: 10.21660/2024.121.g13441.

[23] "COMPARATIVE STUDY ON STATIC AND DYNAMIC ANALYSIS OF STRUCTURES," ERJ. Engineering Research Journal, vol. 39, no. 4, pp. 277–283, Oct. 2016, doi: 10.21608/erjm.2016.66395.

[24] V. Tanuja, P. S. N. Devi, Y. Rakesh, J. Chandu, and J. L. S. Sai, "Analysis and Design of Different Framed Structures G+30 Tall Building Under Dynamic Loading Behaviour," 2025.

[25] Anita Devi, Punita Thakur, and Jainender Sharma, "Comparative study of static and dynamic design analysis of RCC school building," Int. J. Struct. Des. Eng., p. 12, Feb. 2022, doi: https://doi.org/10.22271/27078280.2022.v3.i1a.19.

[26] Y. Nagai, "Investigating parameters governing UHPFRC tensile fatigue behaviour via direct tensile tests on dog-bone shaped specimens," 2025.

[27] C. Yang, Y. Huo, K. Meng, W. Zhou, J. Yang, and Z. Nan, "Fatigue failure analysis of platform screen doors under subway aerodynamic loads using finite element modeling," Engineering Failure Analysis,

vol. 174, p. 109502, June 2025, doi: 10.1016/j.engfailanal.2025.109502.

[28] J.-F. Zhang et al., "Mechanical-property tests on assembled-type light steel modular house," Journal of Constructional Steel Research, vol. 168, p. 105981, May 2020, doi: 10.1016/j.jcsr.2020.105981.

[29] B. Li and C. Shen, "Solid Stress-Distribution-Oriented Design and Topology Optimization of 3D-Printed Heterogeneous Lattice Structures with Light Weight and High Specific Rigidity," Polymers, vol. 14, no. 14, p. 2807, July 2022, doi: 10.3390/polym14142807.

[30] S. N. Patnaik and D. A. Hopkins, "Optimality of a fully stressed design," Computer Methods in Applied Mechanics and Engineering, vol. 165, no. 1–4, pp. 215–221, Nov. 1998, doi: 10.1016/S0045-7825(98)00041-3.

[31] A. T. M. Fathy, S. E. Ghareeb, and Y. Shaban, "Digital Transformation and Design for Maintainability in Industrial Design," Journal of Art, Design and Music, vol. 3, no. 1, Jan. 2024, doi: 10.55554/2785-9649.1031.

[32] Z. Yao, X. Wu, Y. Wu, and X. Wen, "Enhancing Industrial Design Competitiveness: Research and Application of a Machine Tool Industrial Design Decision-Making Method Based on Product Family Architecture and Systematic Evaluation," Applied Sciences, vol. 13, no. 21, p. 11831, Oct. 2023, doi: 10.3390/app132111831.

[33] UNIDO, Ed., Industrializing in the digital age. in Industrial development report, no. 2020. Vienna: UNIDO, 2019.

[34] H. Vijayakumaran, J. B. Russ, G. H. Paulino, and M. A. Bessa, "Consistent machine learning for topology optimization with microstructure-dependent neural network material models," Aug. 27, 2024, arXiv: arXiv:2408.13843. doi: 10.48550/arXiv.2408.13843.

[35] H. Miao, C. Wang, C. Li, W. Song, X. Zhang, and M. Xu, "Nonlinear dynamic modeling and vibration analysis of whole machine tool," International Journal of Mechanical Sciences, vol. 245, p. 108122, May 2023, doi: 10.1016/j.ijmecsci.2023.108122.

[36] H. Wang et al., "Recent advances in machine learning-assisted fatigue life prediction of additive manufactured metallic materials: A review," Journal of Materials Science & Technology, vol. 198, pp. 111–136, Nov. 2024, doi: 10.1016/j.jmst.2024.01.086.

[37] Y. Zhu, J. Zhang, J. Luo, X. Guo, Z. Liu, and R. Zhang, "A Real-Time Remaining Fatigue Life Prediction Approach Based on a Hybrid Deep Learning Network," Processes, vol. 11, no. 11, p. 3220, Nov. 2023, doi: 10.3390/pr11113220.

[38] Y. Liu, C. Liu, X. Gao, and J. Tan, "Multiphysics Finite Element Analysis and Optimization of Load-Bearing Frame for Pure Electric SUVs," Symmetry, vol. 17, no. 7, p. 1143, July 2025, doi: 10.3390/sym17071143.

[39] W. Lin, P. Zhong, X. Wei, L. Zhu, and X. Wu, "Machine tool FEM model correction assisted by dynamic evolution sequence," Sci Rep, vol. 15, no. 1, p. 18789, May 2025, doi: 10.1038/s41598-025-03058-9.

[40] I. U. Hassan, K. Panduru, and J. Walsh, "An In-Depth Study of Vibration Sensors for Condition Monitoring," Sensors, vol. 24, no. 3, p. 740, Jan. 2024, doi: 10.3390/s24030740.

[41] M. Law, P. Gupta, and S. Mukhopadhyay, "Modal analysis of machine tools using visual vibrometry and output-only methods," CIRP Annals, vol. 69, no. 1, pp. 357–360, 2020, doi: 10.1016/j.cirp.2020.04.043.

[42] A. Perisic and B. Perisic, "Digital Twins Verification and Validation Approach through the Quintuple Helix Conceptual Framework," Electronics, vol. 13, no. 16, p. 3303, Aug. 2024, doi: 10.3390/electronics13163303.

[43] A. Kantaros, T. Ganetsos, E. Pallis, and M. Papoutsidakis, "From Mathematical Modeling and Simulation to Digital Twins: Bridging Theory and Digital Realities in Industry and Emerging Technologies," Applied Sciences, vol. 15, no. 16, p. 9213, Aug. 2025, doi: 10.3390/app15169213.

[44] D. Mavrokapnidis, K. Katsigarakis, P. Pauwels, E. Petrova, I. Korolija, and D. Rovas, "A linked-data paradigm for the integration of static and dynamic building data in digital twins," in Proceedings of the 8th ACM International Conference on Systems for Energy-Efficient Buildings, Cities, and Transportation, Coimbra Portugal: ACM, Nov. 2021, pp. 369–372. doi: 10.1145/3486611.3491125.